PCCP

ROYAL SOCIETY OF CHEMISTRY

PAPER

View Article Online
View Journal | View Issue

Cite this: *Phys. Chem. Chem. Phys.*, 2026, **28**, 3588

The limit of the current aromaticity concept

Amnon Stanger, *[a] Jordi Poater [bc] and Yirong Mo [d]

Received 12th October 2025,
Accepted 23rd December 2025

DOI: 10.1039/d5cp03929k

rsc.li/pccp

We investigated the aromatic properties of a set of fifteen cyclic 2π-electron systems and nine 6π-electron charged and neutral systems composed of second-, third-, and fourth-row elements. Three criteria for assessing aromaticity were applied: magnetic (including three variants of the $NICS_{\pi,zz}$ method and current-density analysis), electron-density-based (using the MCI and MCI^{π} indices), and energetic (*via* the BLW method, the simplest form of valence-bond theory). The results reveal that the aromaticity rankings produced by these approaches often diverge, with no clear correlation among the three methods. Aromaticity is not an explicit component of the Hamiltonian or the wavefunction; it is inferred solely through indices and indicators. The absence of correlation between different aromatic measures suggests that establishing aromaticity for systems beyond the second row is intrinsically challenging. More fundamentally, the inconsistencies observed among traditional aromaticity criteria for systems composed of second-row elements in their heavier congeners raise the possibility that aromaticity may not exist beyond the second row. At present, this remains an open question. Noticeably, our findings indicate that NICS values should not be used as a "black box" measure of aromaticity.

Introduction

Aromaticity is one of the fundamental terms in chemistry, yet it is not well defined.[1] The "aromaticity" term stemmed from the attempts to resolve the special properties of benzene, namely, its geometry, its reactivity and its exalted diamagnetic susceptibility. The historic evolution of aromaticity has been described before in several reviews and books, so it is not discussed here.[2] However, it is important to note that the concept of aromaticity has been applied to systems far beyond benzene (for example, polycyclic systems, organometallic systems, transition or even excited states and more) and has given rise to several variations, for example, Möbius aromaticity,[3] Baird aromaticity,[4] 3D-aromaticity, *etc.*[5] Staying within the classical aromaticity concept, the assignment of a compound as aromatic is essentially asking how similar it is to benzene. Does it show bond equalization? Does it have (4n + 2) π electrons? Is it stable relative to a non-aromatic model (which is also not well defined)? Does it show diamagnetic susceptibility exaltation? Does it show induced diatropic ring current under an external magnetic field?

During the years that passed since Hückel's explanation of aromaticity, many of the underlying concepts of aromaticity have been challenged. Some examples are as follows: (a) it was shown that the D_{6h} symmetric structure of benzene is an outcome of the σ frame and the π system is actually more stable as three isolated double bonds (D_{3h}).[6] (b) Systems that do not show even a local minimum on the potential energy surface exhibit a diatropic (aromatic) ring current.[7] (c) A 4n π electron system (phenalenyl cation) shows a diatropic ring current.[8] (d) NMR measurements suggested that $(CO)_3$Cr-benzene is more aromatic than benzene.[9] (e) Cyclobutadiene-dication (a 2π electrons system) is more stable at a non-planar geometry, while the "aromatic" planar geometry is not a minimum on the potential energy surface (with one imaginary frequency).[10] (f) It was shown that paratropicity – usually associated with antiaromaticity – does not necessarily causes destabilization.[11]

The only value of assessing a compound as belonging to a family of compounds (*i.e.*, aromatic) is that chemists know what the expected properties of the compounds are. If the definition is vague and a compound possesses only some of the expected properties, its association with a certain group may be misleading and confusing. The examples above and even more so similar compounds that contain elements beyond the second row (see below) question the validity of the aromaticity concept, especially outside the second row. Thus, the fundamental assessment of aromaticity is based on sp^2 hybridized carbons, which are planar, causing the planar structure of benzene and perfect overlap of p_z orbitals. This concept is valid through the second row, for example, in five-membered rings (furane, pyrrole, and cyclopentadienyl anions) and seven-membered rings (*e.g.*, tropylium cation). However, hybridization is much less important beyond the second row. For

[a] *Schlich Department of Chemistry, Technion, Haifa 3200003, Israel. E-mail: stanger@technion.ac.il*
[b] *Departament de Química Inorgànica i Orgànica & IQTCUB, Universitat de Barcelona, 08028 Barcelona, Spain. E-mail: jordi.poater@ub.edu*
[c] *ICREA, 08010 Barcelona, Spain*
[d] *Department of Nanoscience, Joint School of Nanoscience & Nanoengineering, University of North Carolina at Greensboro, Greensboro, NC 27401, USA. E-mail: Y_MO3@uncg.edu*

example, while the oxygen in water is sp^2 hybridized with an H–O–H angle of 104.5°, the H–S–H bond angle in H_2S is *ca.* 92°, suggesting that each H–S bond is made of an s orbital at the hydrogen and an almost clean p orbital at the sulfur. $H_2Si{=}SiH_2$ significantly deviates from planarity, with an angle of 136.7° between the H–Si–H plane and the Si=Si bond (the respective angle in planar ethylene is 180°) and the respective angle in $H_2Ge{=}GeH_2$ is 115.6°. In brief, if considering that "aromaticity" is based on the similarity to benzene, it is not clear why one should expect the third and fourth row analogs of the second-row aromatics to be aromatic.

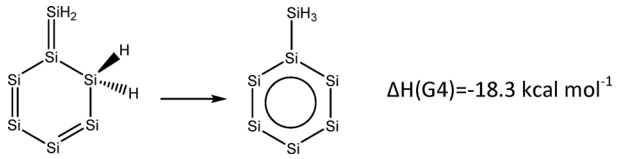

(1)

For experimental (organic) chemists, an aromatic compound or substituent has very specific chemical connotations, for example, special interaction of aromatic amino acids in peptides and proteins or resistance to hydrogenation under conditions that other non-aromatic functional groups are hydrogenated (*e.g.*, olefines and ketones). Hexasilabenzene has equal bond lengths, it is diatropic ($NICS_{zz}$-scan, see Fig. 1, $NICS(1)_{\pi,zz}$ = −33.6 ppm, $\int NICS_{\pi,zz} = -98.9$ ppm) and shows aromatic stabilization energy (eqn (1)).[12] Therefore, one may define it as aromatic, which may mean that hexasilaphenyl can be used in hydrogenation reactions as a substituent, like phenyl. Scheme 1 describes the successive hydrogenation of benzene and hexasilabenzene. While the first hydrogenation of benzene is endothermic (which is the reason for its stabilization under mild hydrogenation conditions), it is exothermic by 24.6 kcal mol^{-1} for hexasilabenzene. The total hydrogenation energy of benzene is less negative than −50 kcal mol^{-1}, while that of hexasilabenzene is −106.7 kcal mol^{-1}. Thus, hexasilaphenyl will be hydrogenated before the intended functional group. Therefore, in this case, defining hexasilabenzene as aromatic is misleading.

One can argue that aromaticity is not a binary property but a quantitative one. Thus, hexasilabenzene may still be aromatic, but less than benzene. The question becomes thus quantitative. If the isomerization energy is a criterion, hexasilabenzene is 55% aromatic relative to benzene. However, if $NICS(1)_{\pi,zz}$ is the criterion, hexasilabenzene is *ca.* 150% aromatic.[13] This question will be dealt with later.

The study that is presented here was initiated by a paper that describes the preparation and properties of an Al-disilacyclopropene derivative.[14] The same authors cited their own work, the synthesis of

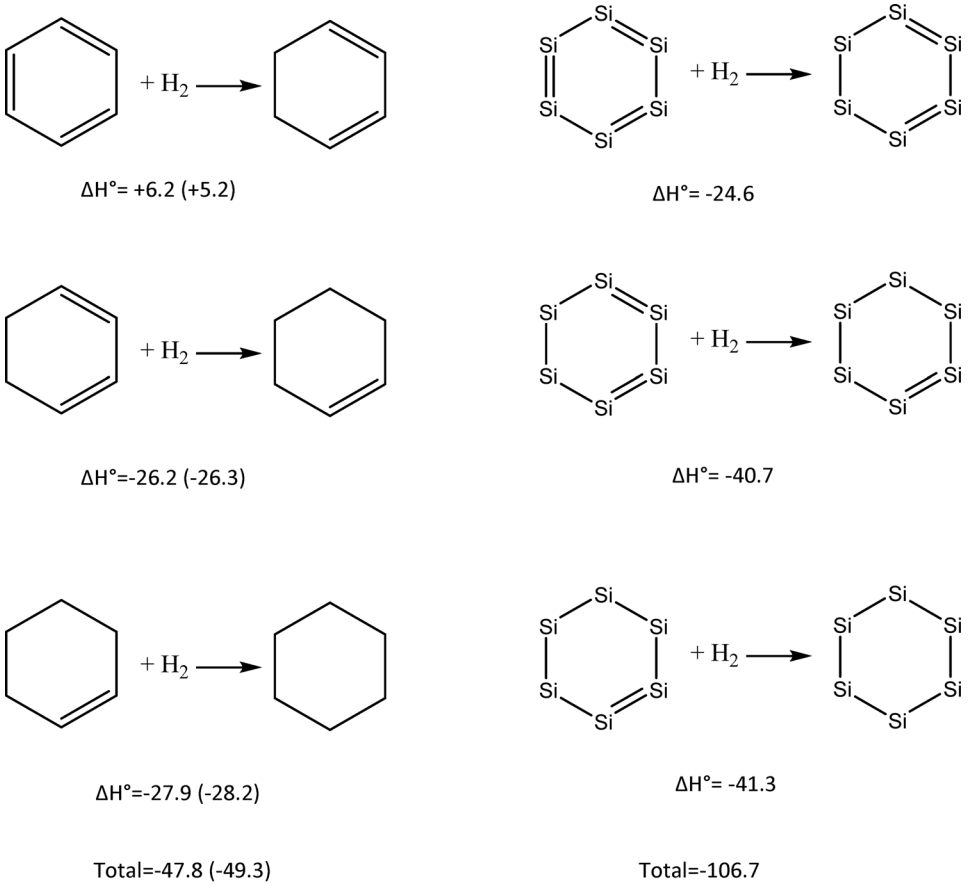

Scheme 1 G4 successive hydrogenation energies (kcal mol^{-1}) of benzene and hexasilabenzene. In parentheses – experimental energies (taken from NIST - NIST Chemistry WebBook (https://webbook.nist.gov/chemistry/)).

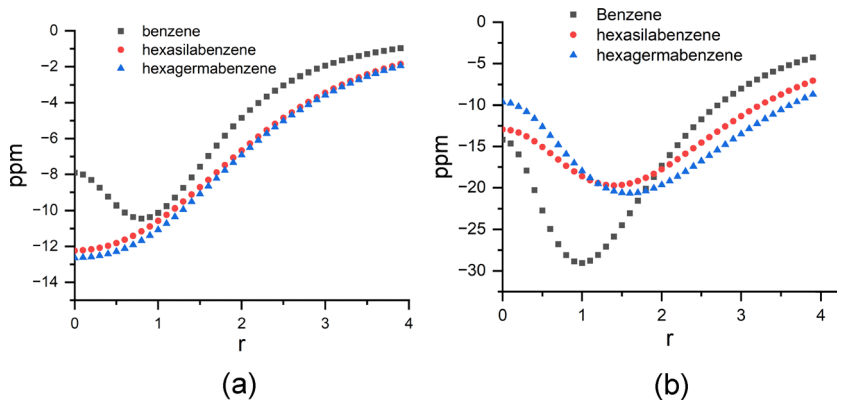

Fig. 1 NICS values (ppm) with respect to the distance (Å) from the molecular plane of benzene, hexasilabenzene and hexagermabenzene. (a, left panel) isotropic NICS. (b, right panel) $NICS_{zz}$.

a B-disilacyclopropene derivative.[15] In both papers, the authors concluded that the studied systems are not aromatic (or weakly aromatic) based on $NICS(1)_{zz}$. The use of $NICS(1)_{zz}$ for such systems is principally a wrong use of the NICS method.

NICS(1) and $NICS(1)_{zz}$ were proposed in order to minimize σ-contaminations. Indeed, when running a NICS-scan[16] on benzene, one finds a minimum of the respective NICS against the distance from the molecular plane at about 1 Å distance. Later, it was shown that these minima in the NICS-scans are a result of paratropic σ-contaminations which decay fast with the distance from the molecular plane.[17] This is true for most second-row systems, so that $NICS(1)_{zz}$ can be used for comparison of diatropicities (aromaticities). However, when the NICS scan is performed for planar hexasilabenzene and hexagermabenzene (both are not minima on the PES, each having one imaginary frequency) the isotropic curve shows no minimum for hexasila- and hexagerma-benzene (Fig. 1a) and the respective minima for the $NICS_{zz}$ are found at 1.4 and 1.6 Å, respectively, from the molecular plane (Fig. 1b). This suggests a very different magnetic behavior for the third and fourth row analogs of benzene. Therefore, comparing $NICS(1)_{zz}$ values for systems made of non-second row elements is meaningless and leads to errors.

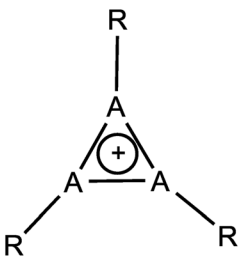

1: A=C. **2**: A=Si. **3**: A=Ge R=H, Me

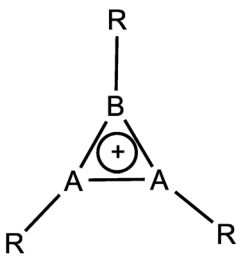

4: A=C, B=Si. **5**: A=C, B=Ge. **6**: A=Si, B=C. **7**: A=Si, B=Ge.
8: A=Ge, B=C. **9**: A=Ge, B=Si. R=H, Me

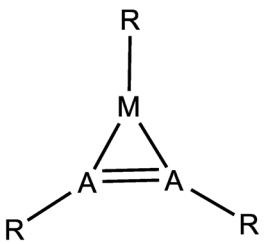

10: A=C, M=B. **11**: A=C, M=Al. **12**: A=Si, M=B. **13**: A=Si, M=Al.
14: A=Ge, M=B. **15**: A=Ge, M=Al. R=H, Me

All the above led us to study systems **1–15**. These systems are all cyclic 2π electron systems made of the second, third and fourth row elements. Three different aromaticity criteria were studied: magnetic (in the form of $NICS_{\pi,zz}$ and current density analysis), electron density (using the MCI method) and energy criteria (with the BLW method, which is the simplest variant of valence bond theory). It is important to note that simple considerations suggest that the second-row derivatives will be more aromatic due to shorter bonds, therefore a better $2p_\pi$ overlap. However, 3p and 4p orbitals are more diffuse than 2p orbitals, so that significant overlap may still be possible in the third and fourth row analogs. The reduced electronegativity in Si and Ge relative to C may help as well in better delocalization. Thus, it is not at all clear that, for example, **1** is more aromatic than **2** or **10** is more aromatic than **15**. The study of the parent systems (*i.e.*, **1–15**, R = H) is discussed in detail here. The results for methylated systems (*i.e.*, **1–15**, R = Me) and the studies of the parent systems at a different computational level are given in the SI since they do not change the general conclusions. An energy-based computational study suggested that the order of aromaticity is **1** > > **2** > **3**.[18]

Computational methods

Systems **1–15** with R–H and R = Me were fully geometrically optimized at the B3LYP-D3/6-311G(d) computational level and the minimal energy geometries were verified with analytical frequency calculations ($N_{imag} = 0$). This level was used for the BLW and MCI analyses.[19] NICS calculations were performed at the GIAO/B3LYP/6-311+G(d) computational level, and the NCS[20] procedure within NBO 7[21] was used for obtaining the CMO-NICS$(r)_{\pi,zz}$ values. Three different analysis procedures were used: CMO-NICS$(1)^{s}_{\pi,zz}$, CMO-NICS$(1)^{L}_{\pi,zz}$ (ref. 22) and CMO-$\int$NICS$_{\pi,zz}$,[23] It is noted that NICS calculations were criticized as suffering from core electrons' influence and electron density effects close to the molecular surface.[24] Therefore, we use here the traditional CMO-NICS$(1)^{s}_{\pi,zz}$ which is based on scanning between 1 and 4 Å from the molecular plane, CMO-NICS$(1)^{L}_{\pi,zz}$ and CMO-$\int$NICS$_{\pi,zz}$, which are based on scanning between 2 and 5 Å from the molecular plane to avoid these local effects.[25] The input for the current density analyses was calculated at the CSGT/B3LYP/6-311+G(d) computational level and analyzed with the SYSMOIC package.[26] All of the above-mentioned QM calculations were performed with the Gaussian 16 package.[27] Block localized wavefunction (BLW)[28] calculations were performed with the GAMESS V30 package[29] to which the BLW code was ported in our lab. MCI calculations were performed with the ESI-3D program[30] using the AIM partition space. Systems s (see below) were calculated at the same computational levels, but the σ-only model[17] was used to assess their tropicities. Energy calculations (eqn (1)–(7)) are based on G4 energies. The crystal structures of derivatives of **2**,[31] **3**,[32] **12**[15] and **13**[14] shows good to excellent agreement with the B3LYP-D3/6-311G(d) optimized structures (a detailed comparison is given in Table S6).

After comparing the current density, NICS, BLW and MCI results, it was decided to repeat the calculations at a different computational level. Thus, geometry optimizations, NICS calculations, BLW analysis and MCI were finally carried out at the M06-2X/def2-qzvp computational level.

Results and discussion

Energy considerations

Aromatic systems are usually associated with extra stability, namely, aromatic stabilization energy (ASE). The definition of ASE is the stabilization relative to a non-aromatic model. This has an inherent problem because this model cannot be defined without any ambiguity and therefore, is prone to controversy. In the cases of **1–3**, the estimation of ASE is even more challenging: The different (unknown) strain energies between **1**, **2** or **3** and their reference systems (*e.g.*, between **1**, cyclopropane and cyclopropene) prevent assessing the ASE. Below are some energy equations that demonstrate these difficulties.

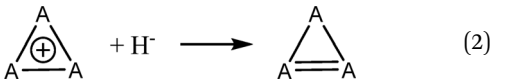

(2)

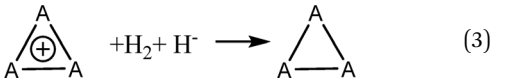

(3)

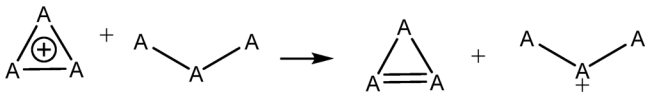

(4)

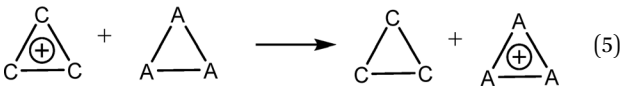

(5)

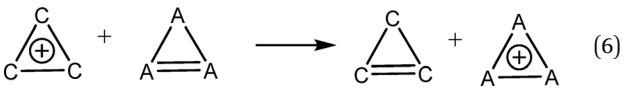

(6)

Table 1 shows the energies of the different equations considered. Eqn (2) for A = C is more exothermic than for A = Si and Ge by 12.4 and 20.2 kcal mol^{-1}, suggesting an ASE order of **1** > **2** > **3**. However, if one considers that the three bonds that are formed are of different types (C–H, Si–H and Ge–H) and that the standard bond energies are 98.7, 76.0 and 68.8 kcal mol^{-1}, respectively, then the ASE order is reversed, namely, the aromaticity order is **3** > **2** > **1**. It is also noted that the hyperconjugation in the right-side molecule of eqn (2) is not considered. Within these numbers, the strain differences between the cation and the double bond containing systems are included. They are unknown and probably very different for the different systems. Eqn (3) gives similar results, with similar

Table 1 ΔH^0 (kcal mol^{-1}) of reactions (2)–(6)

A=/reaction	2	3	4	5	6
C	−232.4	−287.8	28.8		
Si	−220.0	−260.4	29.4	−27.4	13.2
Ge	−212.2	−247.5	27.7	−40.2	−20.9

ASE order when the bond energies are included or not. Eqn (4) resolves the issue of different bond energies and suggests that the ASE is similar for the three systems. However, the strain difference between **1** and **3** and their double-bond containing analogs (the product side) is unknown and so are the hyperconjugative stabilities in the right-side molecules. Due to the larger polarizability in the third and fourth row elements, one may assume that less strain release is involved in the cases of Si and Ge, but the quantitative ASE differences between **1**, **2** and **3** cannot be estimated. Eqn (5) compares **1** directly with **2** and **3** through the saturated ring. Once again, the different bond energies have to be considered, rendering eqn (4) for Si endothermic by 40.7 kcal mol^{-1} and for Ge endothermic by *ca.* 49.5 kcal mol^{-1}. In addition, the different (for C, Si and Ge) strain energy changes between **1–3** and their saturated neutral analogs are unknown but are implicated in these numbers. The best manifestation of this uncertainty is demonstrated in eqn (6). Without the unknowns (as listed above) its results should have been identical to eqn (5). However, when considering the different A–H bond energies, eqn (6) is endothermic by 35.9 and 9.0 kcal mol^{-1} for Si and Ge, respectively.

The use of the methyl-methylene comparison (suggested by Schleyer, eqn (7))[12] is also rather tricky here for a fundamental and practical reason. Fundamentally, it is assumed that the substitution of H for Me (*e.g.*, benzene–toluene) does not significantly change the aromaticity. This is not the case for **1**, where hyperconjugation from the Me group to the ring significantly changes the tropicity (see NICS comparisons between **1-H** and **1-Me**, pages S56 and S57 in the SI). Second, **19–21** are not minima on the potential surface (**19** and **21** open on optimization, **20** is getting a bicyclobutane structure) at the G4 computational level. Thus, this method is also unhelpful when trying to estimate the ASEs in the systems under study. We therefore use the BLW method to estimate the vertical resonance energy. This method is based on the energy difference between a fully delocalized system and the energy when (part of) the delocalization is shut down. In our cases, the interaction that was shut down is the π interaction between the R-M = M-R fragment (M = C, Si, Ge, R = H, Me) and the X-R fragment (X is positively charged C, Si, Ge or uncharged B, Al, R = H, Me) at the optimized geometry of the delocalized systems.

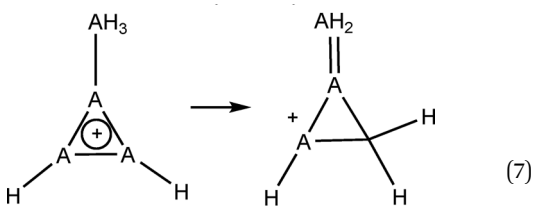

(7)

16: A=C. **17**: A=Si. **18**: A=Ge

19: A=C. **20**: A=Si. **21**: A=Ge

Magnetic studies

Table 2 shows the different NICS values for **1–3**. While for **1** the short-distance-based value is about the same as the long-distance-based value (-11.6 and −10.6 ppm, respectively), as shown by most of second-row systems,[22] the situation in **2** and **3** is very different – NICS(1)$^{L}_{\pi,zz}$ values are about 30% larger (more negative) than NICS(1)$^{s}_{\pi,zz}$. $\int$NICS$_{\pi,zz}$ also suggests that **2** and **3** are much more diatropic than **1**. All this information suggests that the maximally induced currents in **2** and **3** are at larger distances from the molecular plane and are diffused in overall larger distances. This conclusion was tested with current density analysis. Fig. 2 shows the current density plots of **1–3** at different distances from the molecular plane, while all the other plot parameters are identical for all the plots. Clearly, the current density in **1** is maximal at 1.0 a.u. and fades fast with distance. In **2**, the current density is maximal at 1.5 a.u., smaller than in **1**, however, it fades much slower with the distance. In **3**, at 0.5 a.u. the effect of electron density is strong; otherwise, the behavior is similar to that of **2**.

Table 2 NICS values (ppm) of **1–3**

	NICS(1)$^{s}_{\pi,zz}$	NICS(1)$^{L}_{\pi,zz}$	$\int$NICS$_{\pi,zz}$
1	−11.6	−10.6	−23.0
2	−11.9	−15.8	−37.1
3	−12.1	−15.3	−37.4

Another reason for the differences between NICS(1)$^{s}_{\pi,zz}$ and NICS(1)$^{L}_{\pi,zz}$ may be electron density effects[22] that spread over longer distances in third and fourth row elements (*e.g.*, Fig. 2), falsifying the NICS(1)$^{s}_{\pi,zz}$ results.

In summary to this part, tri-Si and tri-Ge cyclopropenium (**2** and **3**, respectively) show larger diatropicities than cyclopropenium. However, due to the sizes of the 2p and 3p orbitals and local electron density effects, these larger diatropicities are found only when looking at distances larger than 1 Å from the molecular plane. The straightforward conclusion is that the tropicity of such systems should not be evaluated at short distance (certainly not by NICS(1)$_{zz}$) but at larger distances.

Heteroatomic cyclopropeniums

Systems **4–9** are studied here. The main differences between them and **1–3** result from (a) the overlap between np and mp orbitals (when $n \neq m$, *e.g.*, 2p with 4p) is smaller than the overlap between the cases of $m = n$ (*i.e.*, **1–3**). (b) The difference between the electronegativities (C > >Ge > Si) causes the electron density to be shifted from the center of the systems. The amount of the electron density shift is probably height dependent. These two differences suggest smaller induced ring currents (*i.e.*, less negative NICS values) and may influence the NICS behavior at different distances from the molecular plane.

Table 3 shows the results. It is rather clear that the combinations of carbon and silicon are the worst in terms of diatropicity. Thus, **4** and **6** are the least diatropic in this series. However, the combination of carbon and germanium (**5** and **8**) is better, showing diatropicity that is only little reduced compared to **3** but certainly enhanced compared to **1**. Interestingly, while **3** shows its diatropicity further away from the molecular plane (NICS(1)$^{s}_{\pi,zz}$ = −12.1, NICS(1)$^{L}_{\pi,zz}$ = −15.3) the situation in **5** is reversed. The differences between the C–Si and C–Ge behavior

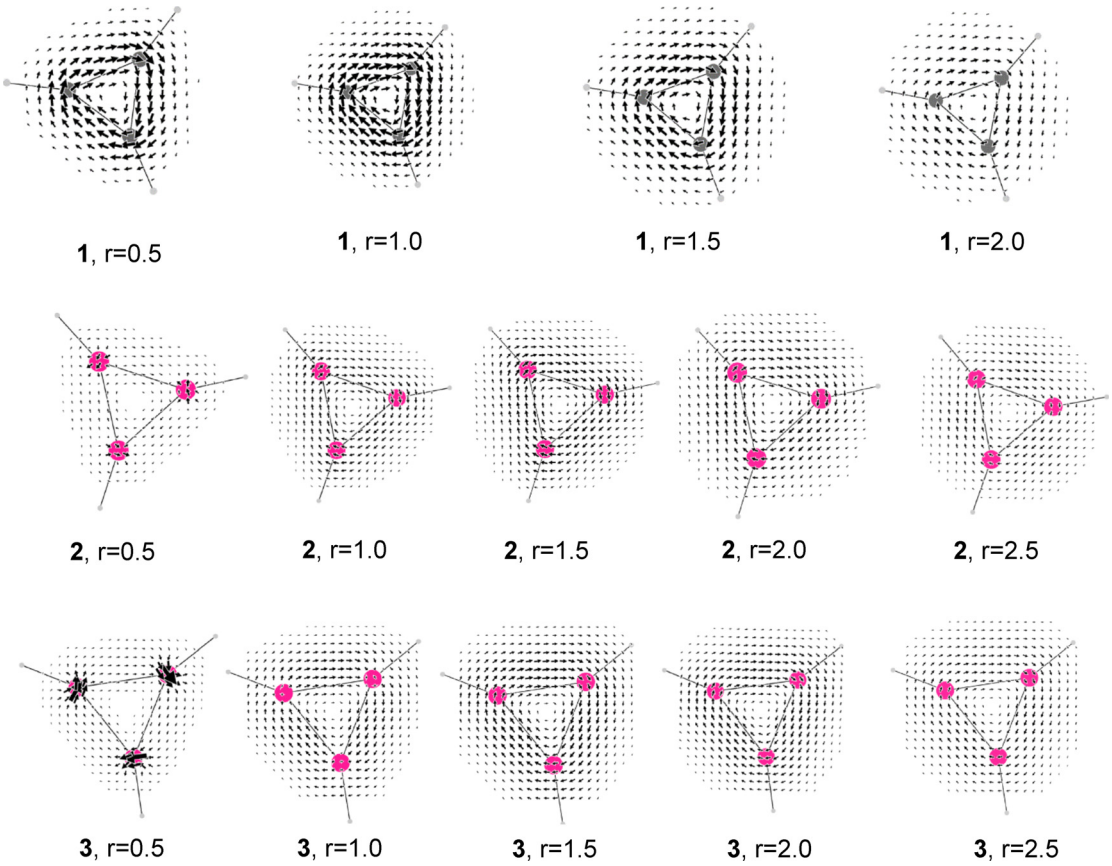

Fig. 2 π-Current densities of **1**, **2** and **3** at different heights (in a.u., *i.e.* a_0 units) from the molecular plane.

Table 3 NICS values (ppm) of **4–9**

	$NICS(1)^{s}_{\pi,zz}$	$NICS(1)^{L}_{\pi,zz}$	$\int NICS_{\pi,zz}$
4	−6.2	−6.3	−13.2
5	−14.8	−11.6	−25.9
6	−8.1	−8.9	−20.2
7	−12.0	−15.0	−36.2
8	−11.3	−13.7	−32.0
9	−12.1	−15.2	−36.8

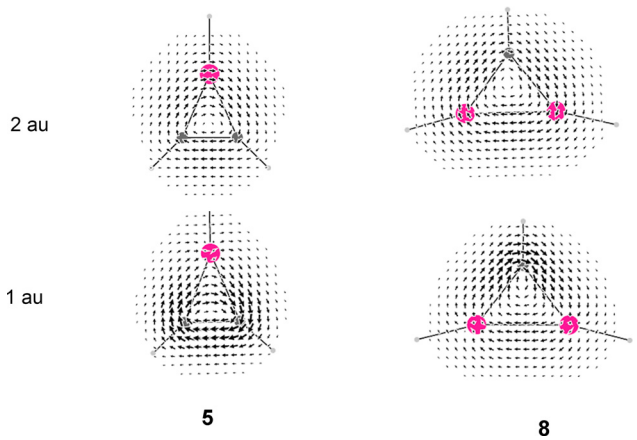

Fig. 3 π-Current densities of **5** and **8** at 1 and 2 a.u. above the molecular plane.

are probably due to the electronegativity – germanium is more electronegative than Si (2.01 and 1.90, respectively), closer to carbon (2.55). It is noted, however, that $\int NICS_{\pi,zz}$ of **4**, **5**, **6** and **8** are reduced relative to **1–3**. For **4** and **6** this is in accordance with the $NICS(1)_{\pi,zz}$ values, but not for **5** and **8**. This can be understood by looking at the current density pictures at 1 and 2 a.u. above the molecular plane (Fig. 3, the full set of the respective current plots are given in Fig. S2).

Apparently, in both derivatives, there is a diatropic current around the carbon atom(s), which is not part of the ring current. This explains why $NICS(1)^{s}_{\pi,zz}$ and $NICS(1)^{L}_{\pi,zz}$ in **5** behave in the opposite way relative to their behavior in **2** and **3** and why $\int NICS_{\pi,zz}$ is not in accordance with the NICS(1) values. However, the mixed Si and Ge derivatives (**7–9**) are (about) as diatropic as their homoatomic derivatives (**2** and **3**).

In general, as expected, the systems that contain atoms of different rows show reduced diatropicity. It is important to note that in such cases, the induced currents are not homogeneous, therefore the best method to estimate their tropicity (in relation to aromaticity) is $\int NICS_{\pi,zz}$ which is influenced less by the non-homogeneity of the induced ring current.

Cyclopropene derivatives (10–15)

Systems **10–15** are three-membered rings with no charge and iso-π-electronic to **1–9** (containing 2π electrons as well). Table 4 lists their different NICS values. In general, they behave like

Table 4 NICS values (ppm) of **10–15**

	$NICS(1)^{s}_{\pi,zz}$	$NICS(1)^{L}_{\pi,zz}$	$\int NICS_{\pi,zz}$
10	−11.1	−11.3	−25.0
11	−9.0	−10.4	−23.8
12	−11.7	−14.4	−35.0
13	−10.6	−13.4	−34.0
14	−12.3	−14.9	−36.4
15	−11.2	−13.9	−35.7

1–3. The carbon-containing derivatives (**10** and **11**) show the smallest diatropicity, $NICS(1)^{s}_{\pi,zz}$ of the Si and Ge containing derivatives (**12–15**) are less negative than $NICS(1)^{L}_{\pi,zz}$ and the values are similar.

After understanding the magnetic behavior of **1–15** it was decided to test the systems using additional criteria of aromaticity.

Block localized wavefunction (BLW) assessments of aromatic stabilization energies (ASE)

Consistent with the VB perspective, the BLW method localizes the movement (delocalization) of π electrons and calculates the energy without the π conjugation. The difference between the fully delocalized (optimized) energy and the electronic localized structure at the same geometry is called vertical resonance energy (VRE). In our cases, the two π electrons are strictly localized between A = A in **1–15** with an empty p_π orbital in A/B/M, effectively disabling the ring circulation. This procedure yields the total resonance energy between the two fragments, the R-M = M-R fragment (with two π electrons) and the $R\text{-}M^{+}$ fragment (M = C, Si, Ge) in **1–9** or R-M′ (M = B, Al) in **10–15**, which is composed of the conjugation energy (*e.g.*, the resonance energy between a double bond and an α-carbenium ion, namely allyl cation) and the aromatic (*i.e.*, extra) stabilization. A suitable conjugated non-aromatic model is required to separate these two energies. Such a perfect model that conjugates two π electrons with the empty p orbital on the $R\text{-}M^{+}$ or R-M' from both sides cannot be devised. However, Model-I (Scheme 2) allows conjugation of the $R\text{-}M^{+}$ or R-M' with two π electrons and Model-II (Scheme 2) conjugates with the $R\text{-}M^{+}$ or R-M' fragment from both sides, but with four π electrons. Therefore, using these models, a range of aromatic resonance energy for each system can be estimated: the differences between the VRE of **1–15** and the VRE of their respective model-I and model-II are the maximum and minimum aromatic resonance energy (or ASE), respectively. The results are given in Table 5. It is rather clear that the BLW aromaticity assignment is very different from the NICS assignment. For example, for **1–3,** the aromaticity assignment by BLW is **1** > > **2** > **3**, the NICS assignment is **2** ≈ **3** > **1**. According to BLW, the four most aromatic systems are **1**, **12**, **10** and **6**, while according to NICS, the most aromatic systems are **2**, **3**, **9** and **14**. It is noted that the VRE of **1–15** linearly correlates with the VRE of model-I and model-II (see Fig. S3) so that for qualitative comparisons, the models are not needed.

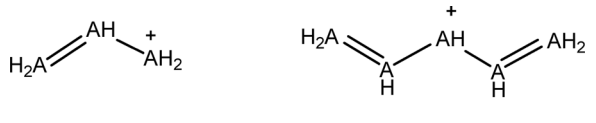

Model-I **Model-II**

Scheme 2 Non-aromatic references for the BLW calculations of ASE (A = C, Si and Ge).

Table 5 BLW vertical resonance energies and aromatic resonance energies (kcal mol^{-1})

	VRE	Model-I	Model-II	MAX. ASE	MIN. ASE
1	−89.79	−55.95	−79.42	−33.84	−10.37
2	−49.58	−31.41	−45.39	−18.17	−4.19
3	−42.18	−29.46	−41.77	−12.72	−0.41
4	−35.46	−18.34	−30.16	−17.12	−5.3
5	−28.91	−15.36	−25.23	−13.55	−3.68
6	−98.84	−77.32	−101.98	−21.52	3.14
7	−45.43	−28.54	−41.24	−16.89	−4.19
8	−88.06	−75.36	−95.57	−12.7	7.51
9	−46.31	−32.62	−46.12	−13.69	−0.19
10	−32.8	−10.97	−19.97	−21.83	−12.83
11	−13.05	−4.54	−8.58	−8.51	−4.47
12	−34.1	−10.95	−23.71	−23.15	−10.39
13	−18.47	−5.03	−10.23	−13.44	−8.24
14	−32.34	−12.04	−25.66	−20.3	−6.68
15	−17.67	−5.82	−11.78	−11.85	−5.89

MCI assessment of aromaticity in 1–15

MCI is an electron-density-based index of aromaticity. The larger it is, the more aromatic the system is. MCI is considered to be not sensitive to the computational level, and it is small for antiaromatic and non-aromatic systems. For example, MCI values for benzene, cyclopentadienyl anions, cyclobutadiene and cyclohexane (at the same computational level) are 0.072, 0.068, 0.009, and 0.000 a.u., respectively (Table 6). Table 6 also lists the MCI values for the parent **1–15**. MCI's order of aromaticity within **1–3** is **1** > **3** > **2**, but the difference is small, rendering them to have almost equal aromaticity. The most aromatic systems, according to MCI, are **1–3**, **7**, **9** and **12** and **14**. Surprisingly, the MCI for these three-membered compounds are much larger than that of benzene. Normalized MCI is considered not to be size-dependent. Thus, the reason must

Table 6 MCI values (in a.u.) for **1–15**. Reference systems are also included for comparison

	MCI	MCI^{π}	MCI^{π}^(1/N)		MCI	MCI^{π}	MCI^{π}^(1/N)
1	0.394	0.286	0.659	**10**	0.185	0.121	0.495
2	0.383	0.251	0.631	**11**	0.124	0.072	0.415
3	0.389	0.264	0.641	**12**	0.378	0.244	0.625
4	0.243	0.163	0.546	**13**	0.230	0.134	0.512
5	0.308	0.209	0.593	**14**	0.368	0.246	0.626
6	0.287	0.173	0.557	**15**	0.249	0.154	0.536
7	0.387	0.260	0.638				
8	0.333	0.232	0.615				
9	0.389	0.269	0.646				
C_6H_6	0.072	0.071	0.644				
$C_5H_5^{-1}$	0.068	0.067	0.583				
C_4H_4	0.009	0.005	0.269				
C_6H_{12}	0.000						

be found in the role of the σ-electrons. It is also possible to compute the π contribution to MCI, *i.e.*, referred to as MCI^{π}, also shown in Table 6. We can notice that in benzene, the π contribution amounts to 99%, however, in the case of **1**, **2** and **3**, MCI^{π} contribution is reduced to 73, 66 and 68%, respectively. Thus, in these systems, *σ* delocalization plays a determinantal role.[33] This percentage ranges from 73% of compound **1** to 60% of **6**. The contribution of Sigma is further increased in those systems enclosing aluminium instead of boron (MCI^{π} contribution between 58 and 62%). For a better comparison between MCI^{π} of three-membered rings with benzene, it is possible to normalize it by means of MCI^{π}^(1/N). These values (Table 6) are similar to values for **1–3** and benzene.

Is aromaticity a valid concept beyond the second row?

The BLW, MCI and NICS studies of the per-methylated systems as well as the studies of **1–15** at the M06-2X/def2-qzvp computational level are given in the SI. These calculations do not change the conclusions that are discussed below.

At this stage, we have presented three quantitative types of BLW-based resonance energies, three types of magnetic criteria, and two electron density criteria (MCI). Fig. 4 shows plots of $NICS(1)^{L}_{\pi,zz}$ against BLW's vertical resonance energies, against MCI^{π} and BLW's vertical resonance energies against MCI^{π}. All the data mentioned above (summarized in Table S4) lead to only one possible conclusion: there is no correlation between different aromaticity indices for **1–15**. There is a vague trend between NICS and MCI (Fig. 4b), but this cannot be considered as a correlation. It seems that what is known about aromaticity in compounds that are made from second row elements is not valid beyond the second row.[34]

The diatropicity in the experimental systems

The "aromaticity" of heavily substituted bora- and alumina-disilacyclopropene was determined by their $NICS(1)_{zz}$ values.[14,15] As shown above (Fig. 1), $NICS(1)_{zz}$ is not a good measure for tropicity outside the second row and, in general, even correct negative NICS values by themselves are not sufficient to determine aromaticity beyond the second row.

The experimental systems are not planar. Thus, $CMO\text{-}NICS_{\pi,zz}$ cannot be computed, and the σ-only model[17] has to be used. This poses a problem since the σ-only model of cyclopropenium is cyclopropane.

Dewar suggested that cyclopropane has σ aromaticity.[35] Since then, there have been a number of papers supporting or disproving this assumption.[35c–f] This disagreement is beyond the scope of this paper, but the diatropicity of cyclopropane has to be considered. Cyclopropane contains three combinations of $\pi(CH_2)$ units, forming the two degenerated π molecular orbitals - HOMO−2 and HOMO−3, and the all-bonding combination HOMO−5. Fig. 5 shows the total current density, the π current density and the σ current density. Obviously, the induced π currents are local, but the σ electrons form a strong induced diatropic current. Fig. 6 shows the

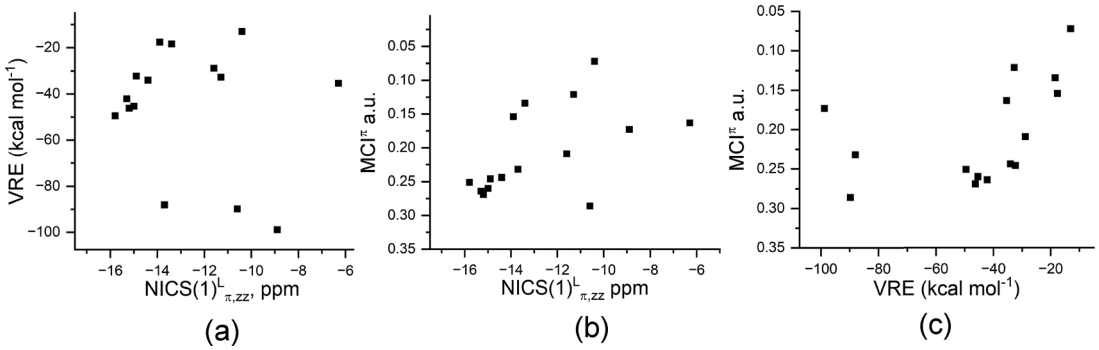

Fig. 4 Plots of aromaticity indices against other aromaticity indices. (a, left panel) $NICS(1)^{L}_{\pi,zz}$ against BLW's VRE. (b, middle panel)) $NICS(1)^{L}_{\pi,zz}$ against MCI. (c, right panel) BLW's VRE against MCI.

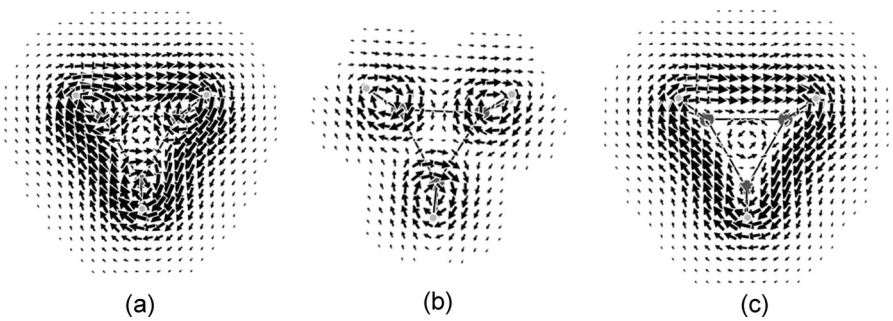

Fig. 5 Current density of cyclopropane at 1 Bohr above the molecular plane. (a, left panel) all electrons. (b, middle panel) π electrons. (c) all the non-π electrons (*i.e.*, σ electrons).

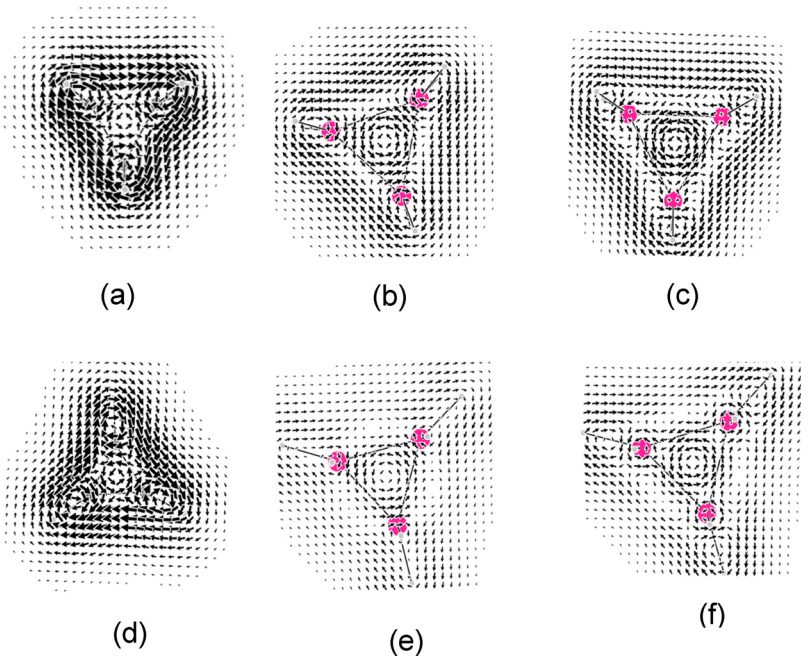

Fig. 6 Current density of cyclopropane (a), trisilacyclopropane (b), trigermacyclopropane (c) and the respective σ-only models of **1** (d), **2** (e) and **3** (f) at 1 Bohr above the molecular plane.

current density of cyclopropane and its tri-sila and tri-germa analogs with the current density of the respective σ-only models. Obviously, the σ-only models of **1–3** are somewhat less diatropic than the respective cyclopropane derivatives, however, they are not ''diatropically silent''. Please also note the difference between MCI and MCI^{π} for **1–15** relative to the respective differences in benzene and cyclopentadienyl anion (Table 6).[36]

The σ-only model approach can be used to assess the tropicity of cyclopropane (and its sila- and germa- derivatives). Thus, in the regular use of the model Hs are bound to atoms containing π bonds, and by that all the π electrons serve now in the σ bonds to H. This mimics the system without π electrons, so subtracting its $NICS_{zz}$ values from the $NICS_{zz}$ values of the (π-containing) system eliminates the σ contribution to NICS, yielding $NICS_{\pi,zz}$ values.[17] The same approach can be used for investigating σ induced currents (*e.g.*, in cyclopropane); protonating the three carbon atoms will use the σ electrons of the CC bonds, producing a model without σ bonds (*e.g.*, similar to three carbenium ions arranged together, where each carbenium ion is placed at the position of the CH_2 unit in cyclopropane). This, of course, can be done for the trisila- and trigerma derivatives. The results of this study (Table 7) are in qualitative agreement with the current density results.

Table 8 shows the CMO-$NICS(1)_{\pi,zz}$ and the σ-only (SOM)-$NICS(1)_{\pi,zz}$ values calculated from the scans of 1–4 Å (S) and 2–5 Å (L) of **1–3** and **10–15**. In general, for the second row containing systems (**1** and **10**), at the low scan, the SOM is less negative by *ca.* 3 ppm and at high scan by *ca.* 10 ppm. For the third row systems (**2** and **13**), at the low and high scans, the SOM is more negative by 10 and 13 ppm, respectively.

Table 7 σ-Only $NICS_{zz}$ values (ppm, see text) of cyclopropane, trisilacyclopropane and trigermacyclopropane

	$NICS(1)^{S}_{zz}$	$NICS(1)^{L}_{zz}$	$\int NICS_{zz}$
Cyclopropane	−11.2	−9.2	−21.3
Trisilacyclopropane	−9.3	−10.7	−30.4
Trigermacyclopropane	−5.4	−6.6	−22.5

Table 8 Comparison of CMO-$NICS(1)_{\pi,zz}$ and σ-only-$NICS(1)_{\pi,zz}$ for **1–3** and **10–15**

	CMO-$NICS(1)^{S}_{\pi,zz}$	σ-only-$NICS(1)^{S}_{\pi,zz}$	CMO-$NICS(1)^{L}_{\pi,zz}$	σ-only-$NICS(1)^{L}_{\pi,zz}$
1	−11.6	−8.0	−10.6	−0.1
2	−11.9	−21.5	−15.8	−28.6
3	−12.1	−22.7	−15.3	−29.6
10	−11.1	−9.8	−11.3	−1.0
11	−9.0	−13.1	−10.4	−17.6
12	−11.7	−19.9	−14.4	−26.2
13	−10.6	−20.9	−13.4	−27.3
14	−12.3	−19.9	−14.9	−25.3
15	−11.2	−22.1	−14.0	−26.9

The fourth row system (**3**) and the combination of Ge and Al (**15**) show at low and high scans that SOM is more negative by 10.5–11 and 13–14 ppm, respectively. The mixed second-third and second-fourth row systems show mixed results.

For the calculations of the experimental systems, a close computational model was chosen, see Scheme 3. The NICS data are given in Table 9. For the parent systems, the diatropicity is reduced by *ca.* 20% (for **2** and **3**) to 50% (for SOM-$NICS(1)^{L}_{\pi,zz}$). Interestingly, the diatropicity is considerably enhanced in **10**, but for **11–15** it is reduced but *ca.* 20–30%. Please note that

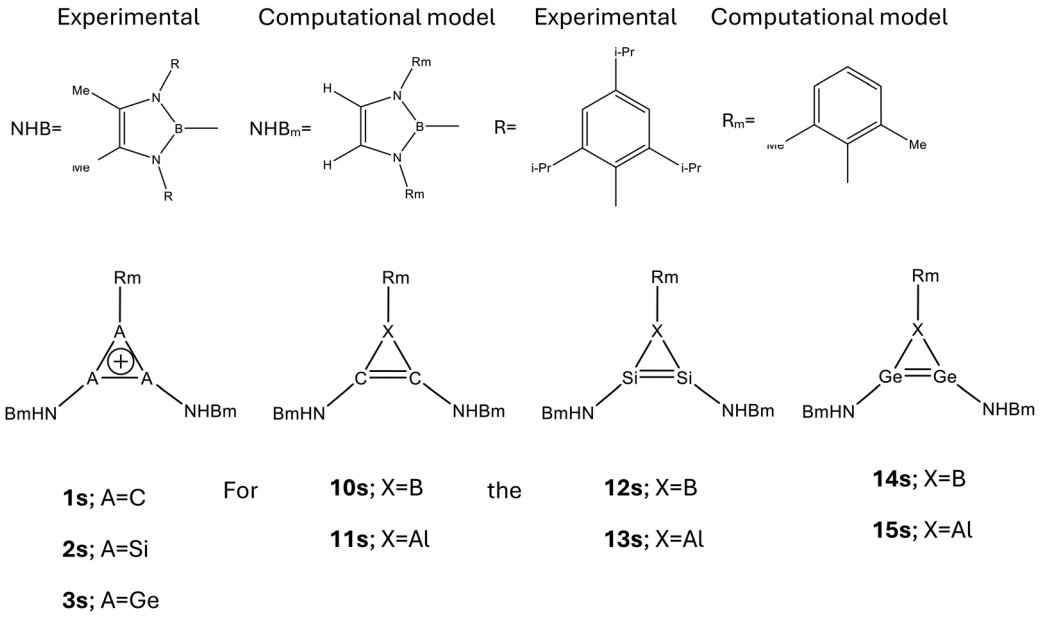

Scheme 3 Definition of the experimental substituents and their computational models.

Table 9 σ-Only-NICS$_{\pi,zz}$ of **1–3** and **10–15** and their respective substituted S derivatives

	S, parent[a]	S, s-system[b]	L, parent[c]	L, s-system[d]
1	−8.0	−2.7	−0.1	−0.1
2	−21.5	−16.5	−28.6	−22.6
3	−22.7	−16.8	−29.6	−22.0
10	−9.8	−8.2	−1.0	−1.1
11	−13.1	−9.4	−17.6	−11.6
12	−19.9	−8.4	−26.2	−11.8
13	−20.9	−16.6	−27.3	−23.1
14	−19.9	−14.8	−25.3	−19.0
15	−22.1	−16.6	−26.9	−22.4

[a] σ-only-NICS$(1)^{s}_{\pi,zz}$ of the parent systems. [b] σ-only-NICS$(1)^{s}_{\pi,zz}$ of the substituted S systems (see Scheme 2). [c] σ-only-NICS$(1)^{L}_{\pi,zz}$ of the parent systems. [d] σ-only-NICS$(1)^{L}_{\pi,zz}$ of the substituted S systems (see Scheme 2).

both experimental systems (**12** and **13**) are more diatropic than **1** – the prototype of 2π-electron aromatic systems.

6-π electron systems

All the systems that are studied so far are 3-centers-2π systems. In order to make sure that our conclusions are not specific for this class of systems, we have studied 6-π electron systems with different ring sizes; cyclopentadienyl anion, benzene, tropylium cation and their sila and germa analogs.

These systems pose a problem for the comparison of the methods. While NICS$_{\pi,zz}$ can be computed for planar (using CMO-NICS) and non-planar (using the σ-only model)[37] systems, BLW and MCI$^{\pi}$ can be carried out only for planar systems. All the sila and germa derivatives are not planar. Thus, the comparison here is between the three methods for the D_nh-symmetric systems (n = 5,6,7) and between σ-only-NICS$_{\pi,zz}$ and MCI. Table S5 describes the energy differences between the fully optimized structures and the D_nh structures and the number of imaginary frequencies for the latter.

Table 10 NICS$(1)_{\pi,zz}$ and $\int$NICS$_{\pi,zz}$ (thw two right columns) for D_{5h}-cyclopentadienyl anions, D_6h-benzene and D_7h-tropylium cations and their Si and Ge analogs

	CMO^{s}	σ-only^{s}	CMO^{L}	σ-only^{s}	∫CMO	∫σ-only
CP^-	−29.3	−27.4	−32.4	−28.3	−77.9	−67.1
Si_5-CP^-	−22.8	−30.3	−29.9	−32.1	−89.5	−90.8
Ge_5-CP^-	−24.6	−32.2	−30.2	−32.7	−92.6	−93.8
benzene	−29.7	−34.8	−33.9	−34.4	−82.2	−82.4
Si_6-benzene	−23.0	−29.6	−29.3	−33.6	−90.9	−98.0
Ge_6-benzene	−24.5	−32.3	−29.7	−33.6	−94.7	−105.9
Tropylium$^+$	−28.9	−32.4	−33.5	−33.5	−84.1	−83.0
Si_7-Tropylium$^+$	−21.9	−23.7	−26.9	−28.6	−88.9	−89.7
Ge_7-Tropylium$^+$	−23.1	−25.4	−27.5	−29.6	−93.3	−95.0

The σ-only model was developed for the 2nd row atoms. Thus, it should be tested for the Si and Ge derivatives. Table 10 compares different NICS values. Interestingly, the NICS$(1)^{s}_{\pi,zz}$ and NICS$(1)^{L}_{\pi,zz}$ that are obtained from the σ-only model are more similar than those obtained from CMO. This is probably due to the cancellation of the electron density effects close to the molecular plane. In any event, within less than ±10% the CMO and σ-only NICS$_{\pi,zz}$ values are equal, which reassures that they can be used for the non-planar systems.

For the BLW studies, the π electrons are always divided into one block with two π electrons (ethylene-like) and one block of 4 π electrons (allyl anion-like for the cyclopentadienyl anion derivatives, 1,3-butadiene-like for the benzene derivatives and pentadienyl cation-like for the tropylium cation derivatives). The non-aromatic models that were used for obtaining the ASE were always the respective open-chain derivatives with the respective blocks. Table 11 lists the BLW's VRE and ASE and all the MCI-based data for the D_nh structures. Fig. 7 shows some plots of the NICS, MCI$^{\pi}$ and BLW's ASE for the D_nh symmetrical systems. As in the case of the three-membered

Table 11 BLW energies (kcal mol^{-1}) and MCI parameters (a.u.) for the 6 π electron systems

	VRE	ASE	MCI	MCI$^{\pi}$	MCI$^{\pi}$^(1/N)
CP^-	−90.84	−26.77	0.068	0.067	0.582
Si_5-CP^-	−50.83	−10.05	0.054	0.053	0.555
Ge_5-CP^-	−47.04	−10.36	0.067	0.066	0.580
Benzene	−60.24	−43.81	0.072	0.071	0.644
Si_6-benzene	−31.35	−22.18	0.051	0.051	0.609
Ge_6-benzene	−29.42	−20.83	0.067	0.067	0.637
Tropylium$^+$	−133.97	−44.42	0.057	0.057	0.665
Si_7-Tropylium$^+$	−71.79	−21.42	0.038	0.038	0.627
Ge_7-Tropylium$^+$	−68.12	−21.51	0.052	0.052	0.656

Table 12 NICS (ppm) and MCI (a.u.) parameters for the fully optimized systems

	NICS(1)^S	NICS(1)^L	∫NICS	MCI
CP^-	−27.4	−28.3	−67.1	0.068
Si_5-CP^-	−21.0	−25.2	−70.9	0.025
Ge_5-CP^-	−14.7	−18.7	−54.2	0.005
Benzene	−34.8	−34.4	−82.4	0.072
Si_6-benzene	−27.5	−33.6	−97.9	0.035
Ge_6-benzene	−24.3	−31.1	−92.0	0.014
Tropylium$^+$	−32.4	−33.5	−83.0	0.057
Si_7-Tropylium$^+$	−23.3	−28.3	−88.4	0.036
Ge_7-Tropylium$^+$	−21.4	−26.9	−86.1	0.024

rings (Fig. 4), one may see a trend in the NICS *vs.* MCS$^{\pi}$ and against ASE, but these cannot be considered as correlations.

The NICS$_{\pi,zz}$ and MCI data for the fully optimized systems are given in Table 12. The diatropicity and the MCI are reduced compared with the planar systems (see Tables 10 and 11), in qualitative agreement with the energy difference between the D_nh and the optimized structures (Table S5). Yet, there is still no correlation between NICS and MCI (Fig. 8).

Finally, with some limitations, it is possible to combine all the results of all the principal systems that are studied here – **1–15** and the nine cyclopentadienyl anion, benzene, tropylium cation and their sila- and germa- derivatives. To do that MCI$^{\pi}$^(1/N) has to be used (MCI and MCI$^{\pi}$ are sensitive to the size), all the systems have to be planar – allowing the use of BLW analysis, and the ASE that is used is the ''MAX. ASE'' (Table 5) to be coherent with the ASE for the 6 π electron systems. Fig. 9 shows the results, reinforcing the lack of correlation between the three aromaticity parameters.

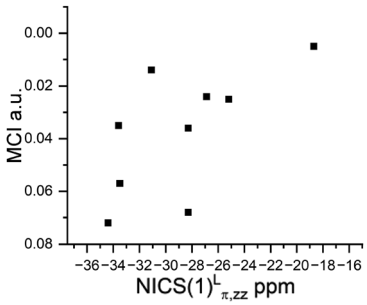

Fig. 8 A plot of NICS(1)$^L_{\pi,zz}$ against MCI for the optimized structures of the 6 π electron systems discussed.

Summary and conclusions

Fifteen 2π-electron systems and nine 6π-electron systems constructed from second-, third-, and fourth-row elements were examined using magnetic criteria (three variants of NICS and current-density analysis), BLW calculations to assess aromatic resonance energy, and electron-density criteria (MCI and MCI$^{\pi}$). These represent three independent aromaticity metrics, yet in the present study, they clearly contradict one another.

It is important to note that neither the wavefunction nor the Hamiltonian contains any explicit ''aromatic'' component. Consequently, the identification and quantitative assessment of aromaticity rely entirely on indices and indicators. We have shown here that these indicators are not reliable for the types of systems studied. Thus, the logic commonly applied to second-row element compounds, namely, evaluating one or two indices (for example, magnetic and geometric), assigning aromaticity, and then inferring associated properties such as kinetic stability, cannot be extended to these heavier-element systems. Aromaticity is a functional definition. Thus, in such cases, labeling a compound ''aromatic'' becomes redundant, as each property must instead be evaluated independently.

This raises a more fundamental question: because aromaticity can only be inferred through indices, and since no available indicator can be independently validated against another (*e.g.*,

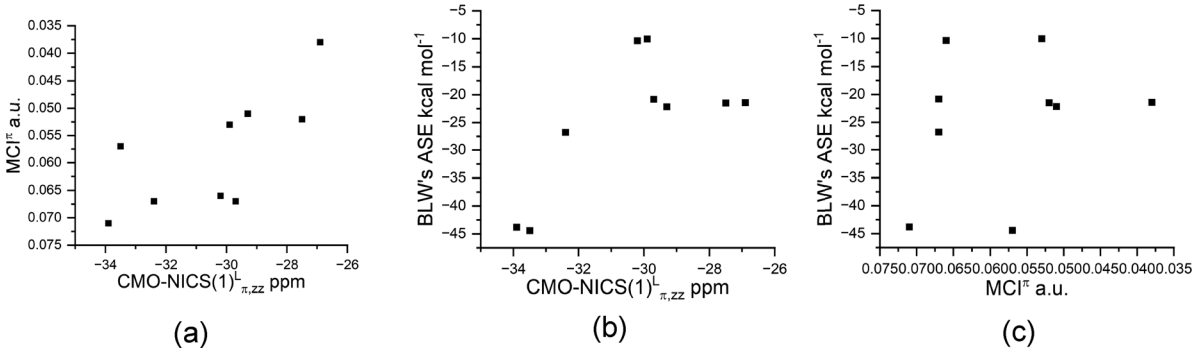

Fig. 7 Plots of CMO-NICS(1)$_{\pi,zz}$ against (a, left panel) MCI$^{\pi}$ and (b, middle panel) ASE and (c, right panel) MCI$^{\pi}$ against ASE.

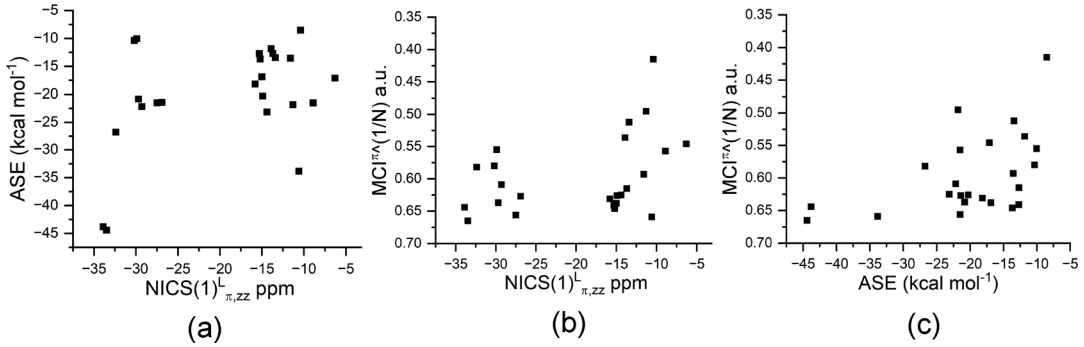

Fig. 9 Plots of $NICS(1)^{L}_{\pi,zz}$ against (a, left panel) ASE and (b, middle panel) MCI^{π}^(1/N) and (c, right panel) ASE against MCI^{π}^(1/N).

magnetic *vs.* energetic criteria), how can we be certain that aromaticity exists at all in these systems? To the best of our knowledge, no answer currently exists.

We also demonstrate that NICS values should not be used as a "black box." Applying, for instance, $NICS(1)_{zz}$ as a universal aromaticity measure to compounds containing elements beyond the second row frequently leads to erroneous conclusions about the nature and magnitude of ring currents (tropicity).

Conflicts of interest

There are no conflicts to declare.

Data availability

Supplementary information (SI): file including optimized geometries, additional NICS data, current density plots, VRE plots, results and discussion on the per-methylated systems, NICS, MCI and VRE data at the M06-2X/def2-qzvp level, summary of all the results at the B3LYP/6-311G(d) level for the parent systems, data of the 6π electrons systems and explanation of the NICS methods. See DOI: https://doi.org/10.1039/d5cp03929k.

Acknowledgements

J. P. thanks the Spanish Ministerio de Ciencia, Innovación y Universidades (PID2022-138861NB-I00 and CEX2021-001202-M).

References

1 There is no "aromatic part" in the Hamiltonian, nor in the wave function.
2 (*a*) *Aromaticity modern computational methods and applications*, ed I. Fernández, Elsevier, 2021, ISBAN 978-0-12-822723-7; (*b*) M. Solà, A. I. Boldyrev, M. K. Cyrański, T. M. Krygowski and G. Merino, *Aromaticity and antiaromaticity. Concepts and applications*, John Wiley & Sons, Ltd., 2023, ISBN: 9781119085898; (*c*) *Chem. Rev.*, 2001, **101**(5); (*d*) *Chem. Rev.*, 2005, **105**(10); (*e*) *Chem. Soc. Rev.*, 2015, **44**(18).
3 (*a*) H. S. Rzepa, *Chem. Rev.*, 2005, **105**, 3697–3715; (*b*) X. Lin, W. Wu and Y. Mo, *J. Am. Chem. Soc.*, 2023, **145**, 8107–8113.
4 (*a*) *J. Phys. Org. Chem.*, 2023, **36**(1); (*b*) J. Yan, T. Slanina, J. Bergman and H. Ottosson, *Chem. – Eur. J.*, 2023, **29**, e202203748; (*c*) H. Ottosson, *Nat. Chem.*, 2022, **4**, 969–971.
5 (*a*) Gl Merino, M. Sola, I. Fernandez, C. Foroutan-Nejad, P. Lazzeretti, G. Frenking, H. L. Anderson, D. Sundholm, F. P. Cossio, M. A. Petrukhina, J. Wu, J. I. Wu and A. Restrepo, *Chem. Sci.*, 2023, **14**, 5569–5576; (*b*) O. El Bakouri, D. W. Szczepanik, K. Jorner, R. Ayub, P. Bultinck, M. Sola and H. Ottosson, *J. Am. Chem. Soc.*, 2022, **144**, 8560–8575; (*c*) J. Poater, C. Viñas, M. Sola and F. Teixidor, *Nat. Commun.*, 2022, **13**, 3844.
6 (*a*) S. C. A. H. Pierrefixe and F. M. Bickelhaupt, *Chem. – Eur. J.*, 2007, **13**, 6321–6328; (*b*) A. Stanger, *J. Phys. Chem. A*, 2008, **112**, 12849–12854; (*c*) S. Shaik, A. Shurki, D. Danovich and P. C. Hiberty, *Chem. Rev.*, 2001, **101**, 1501–1539; (*d*) A. Stanger and K. P. C. Vollhardt, *J. Org. Chem.*, 1988, **53**, 4889–4890; (*e*) A. Stanger, *J. Am. Chem. Soc.*, 1991, **113**, 8277–8280.
7 L. Zhao, R. Grande-Aztatzi, C. Foroutan-Nejad, J. M. Ugalde and G. Frenking, *ChemistrySelect*, 2017, **2**, 863–870.
8 M. K. Cyrański, R. W. A. Havenith, M. A. Dobrowolski, B. R. Gray, T. M. Krygowski, P. W. Fowler and L. W. Jenneskens, *Chem. – Eur. J.*, 2007, **13**, 2201–2207.
9 (*a*) R. H. Mitchell, P. Zhou, S. Venugopalan and T. W. Dingle, *Am. Chem. Soc.*, 1990, **112**, 7812; (*b*) R. H. Mitchell, Y. Chen, N. Khalifa and P. Zhou, *J. Am. Chem. Soc.*, 1998, **120**, 1785; (*c*) R. H. Mitchell, Z. Brkic, D. J. Berg and T. M. Barclay, *J. Am. Chem. Soc.*, 2002, **124**, 11983; (*d*) A. Stanger, *Can. J. Chem.*, 2017, **95**, 263–270.
10 L. H. Körner, L. Phong, R. Puchta, A. Stanger and M. Tamm, *Chem. – Eur. J.*, 2022, **28**, e202202737.
11 C. Foroutan-Nejad, *J. Org. Chem.*, 2023, **88**, 14831–14835.
12 According toP. V. R. Schleyer and F. Pühlhofer, *Org Lett.*, 2002, **4**, 2873–2876The respective energy for benzene (through toluene isomerization) is −33.2 kcal mol^{-1}.
13 The data for the %aromaticity are shown at the result and discussion section.
14 L. Guo, J. Zhang and C. Cui, *J. Am. Chem. Soc.*, 2023, **145**, 27911–27915.
15 M. Tian, J. Zhang, L. Guo and C. Cui, *Chem. Sci.*, 2021, **12**, 14635–14640.

16 A. Stanger, *J. Org. Chem.*, 2006, **71**, 883–893.
17 A. Stanger, *J. Org. Chem.*, 2010, **75**, 2281–2288.
18 I. Ferández, M. Duvall, J. I.-C. Wu, P. V. R. Schleyer and G. Frenking, *Chem. – Eur. J.*, 2011, **17**, 2215–2224.
19 P. Bultinck, R. Ponec and S. Van Damme, *J. Phys. Org. Chem.*, 2005, **18**, 706–718.
20 J. A. Bohmann, T. C. Farrar and F. Weinhold, *J. Chem. Phys.*, 1997, **107**, 1173–1184.
21 E. D. Glendening, C. R. Landis and F. Weinhold, *J. Comput. Chem.*, 2019, **40**, 2234–2241.
22 A. Stanger, *ChemPhysChem*, 2023, **24**, e202300080.
23 A. Stanger, *J. Phys. Chem. A*, 2019, **123**, 3922–3927.
24 (*a*) M. Orozco-Ic, N. D. Charistos, A. Muñoz-Castro, R. Islas, D. Sundholm and G. Merino, *Phys. Chem. Chem. Phys.*, 2022, **24**, 12158–12166; (*b*) M. Orozco-Ic, L. Soriano-Agueda, D. Sundholm, E. Matito and G. Merino, *Chem. Sci.*, 2024, **15**, 12906–12921.
25 Per a reviewer request, an elaborated discussion about the NICS methods (including references) is given in the SI pages S65-S67.
26 G. Monaco, R. Summa and R. Zanasi, Program Package for the Calculation of Origin-Independent Electron Current Density and Derived Magnetic Properties in Molecular Systems, *J. Chem. Inf. Model.*, 2021, **61**, 270–283.
27 M. J. Frisch, G. W. Trucks, H. B. Schlegel, G. E. Scuseria, M. A. Robb, J. R. Cheeseman, G. Scalmani, V. Barone, G. A. Petersson, H. Nakatsuji, X. Li, M. Caricato, A. V. Marenich, J. Bloino, B. G. Janesko, R. Gomperts, B. Mennucci, H. P. Hratchian, J. V. Ortiz, A. F. Izmaylov, J. L. Sonnenberg, D. Williams-Young, F. Ding, F. Lipparini, F. Egidi, J. Goings, B. Peng, A. Petrone, T. Henderson, D. Ranasinghe, V. G. Zakrzewski, J. Gao, N. Rega, G. Zheng, W. Liang, M. Hada, M. Ehara, K. Toyota, R. Fukuda, J. Hasegawa, M. Ishida, T. Nakajima, Y. Honda, O. Kitao, H. Nakai, T. Vreven, K. Throssell, J. A. Montgomery Jr., J. E. Peralta, F. Ogliaro, M. J. Bearpark, J. J. Heyd, E. N. Brothers, K. N. Kudin, V. N. Staroverov, T. A. Keith, R. Kobayashi, J. Normand, K. Raghavachari, A. P. Rendell, J. C. Burant, S. S. Iyengar, J. Tomasi, M. Cossi, J. M. Millam, M. Klene, C. Adamo, R. Cammi, J. W. Ochterski, R. L. Martin, K. Morokuma, O. Farkas, J. B. Foresman and D. J. Fox, *Gaussian 16, Revision C.01*, Gaussian Inc., Wallingford CT, 2019.
28 (*a*) Y. Mo, *J. Phys. Chem. A*, 2009, **113**, 5163–5169; (*b*) Y. Mo and S. D. Peyerimhoff, *J. Chem. Phys.*, 1998, **109**, 1687–1697; (*c*) Y. Mo, L. Song and Y. Lin, *J. Phys. Chem. A*, 2007, **111**, 8291–8301.
29 M. W. Schmidt, K. K. Baldridge, J. A. Boatz, S. T. Elbert, M. S. Gordon, J. H. Jensen, S. Koseki, N. Matsunaga, K. A. Nguyen, S. Su, T. L. Windus, M. Dupuis and J. A. Montgomery Jr, General atomic and molecular electronic structure system, *J. Comput. Chem.*, 1993, **14**(11), 1347–1363.
30 E. Matito, M. Sola, P. Salvador and M. Duran, *Faraday Discuss.*, 2007, **135**, 325–345.
31 M. Ichinohe, M. Igarashi, K. Sanuki and A. Sekiguchi, *J. Am. Chem. Soc.*, 2005, **127**, 9978–9979.
32 (*a*) A. Sekiguchi, M. Tsukamoto and M. Ichinohe, *Science*, 1997, **275**, 60–61; (*b*) A. Sekiguchi, M. Tsukamoto, M. Ichinohe and N. Fukaya, *Phosphorus, Sulfur Silicon Relat. Elem.*, 1997, **124**(125), 323–329; (*c*) M. Ichinohe, N. Fukaya and A. Sekiguchi, *Chem. Lett.*, 1998, 1045–1046; (*d*) A. Sekiguchi, N. Fukaya and M. Ichinohe, *Phosphorus, Sulfur Silicon Relat. Elem.*, 1999, **150**(151), 59–68; (*e*) A. Sekiguchi, N. Fukaya, M. Ichinohe and Y. Ishida, *Eur. J. Inorg. Chem.*, 2000, 1155–1159.
33 N. P. Vedin, J. M. Toldo, S. Escayola, S. Radenković, M. Sola and H. Ottosson, *J. Org. Chem.*, 2025, **90**, 9743–9756.
34 R. Hoffmann, *Perspective*, PERSPECTIVE.pdf (https://roaldhoffmann.com/sites/default/files/fromd6/PERSPECTIVE.pdf).
35 (*a*) M. J. S. Dewar and L. McKee, *Pure Appl. Chem.*, 1980, **52**, 1431–1441; (*b*) M. J. S. Dewar, *Bull. Soc. Chim. Belg.*, 1979, **88**, 957–967; (*c*) I. A. Popov, A. A. Starikova, D. V. Steglenko and A. I. Boldyrev, *Chem. – Eur. J.*, 2018, **24**, 292–305; (*d*) D. Moran, M. Manoharan, T. Heine and P. V. R. Schleyer, *Org. Lett.*, 2003, **5**, 23–26; (*e*) S. Pelloni, P. Lazzeretti and R. Zanasi, *J. Phys. Chem. A*, 2007, **111**, 8163–8169; (*f*) W. Wu, B. Ma, J. I.-C. Wu, P. V. R. Schleyer and Y. Mo, *Chem. – Eur. J.*, 2009, (15), 9730–9736.
36 The special properties of cyclopropane are well manifested in its reactivity. For a recent review seeN. Wang, J.-X. Zhao and J.-M. Yue, *Org. Chem. Front.*, 2025, **12**, 2439–2456.
37 See SI for detailed explanations of the methods.

